Hindawi
Shock and Vibration
Volume 2021, Article ID 8813115, 9 pages
https://doi.org/10.1155/2021/8813115

Research Article

Uniaxial Compression Mechanical Analysis of Cylindrical Rock Specimens Based on Space Axisymmetric Problem

Jianguang Li, Yanchun Wang, and Chuanqi Su

College of Mechanical and Electronic Engineering, Qingdao University of Science and Technology, Qingdao, China

Correspondence should be addressed to Jianguang Li; qingdaokeda@126.com

Received 13 August 2020; Revised 6 February 2021; Accepted 18 March 2021; Published 30 March 2021

Academic Editor: Zengshun Chen

The common failure forms in the uniaxial compression test of standard cylindrical rock specimens are symmetric cone failure and splitting failure. In the past, two kinds of failure forms were explained from the plane problems of elasticity theory. However, there was a lack of research based on space problems. In this paper, based on spatial axisymmetric elastic mechanics theory, three-dimensional stress function is constructed for the cylindrical rock specimen under uniform axial compression by adopting the semi-inverse method. According to the stress function, the stress components and the principal stress are deduced when considering the end effect. The failure form is speculated, which can well explain the two common types of damage in uniaxial compression. This work may enrich the basic research of rock mechanics.

1. Introduction

As we all know, uniaxial compression experiment is the most common type of experiment to understand the mechanical properties of certain kinds of rocks. In various international standards, national standards, local standards, and industrial standards, there are clear test procedures, and the experimental results have become the classic textbook content. The two corresponding types of typical failure, i.e., split failure and symmetric cone failure, impressed people deeply. Traditionally, it is believed that the failure mechanism is related to the end effect of the compression head of the testing machine. But this explanation is not detailed and thorough enough from the view point of mathematical mechanics model. Some researchers tried to use the theory of elastic mechanics to derive the stress function. However, most of them are confined to the two-dimensional space, and most of the three-dimensional stress functions used to solve the rock-related problems are only based on fuzzy theoretical reasoning [1, 2], which lacks the applicability extension. In reference [1], the two-dimensional Airy stress function of cylindrical rock specimens under uniform load was given. In this paper, based on further derivation on the theory of spatial axisymmetry [3–5], the three-dimensional stress function and stress components of a standard cylindrical rock specimen under uniform axial load will be given on the basis of reference to predecessors' experience [6–12], and the destruction mechanism of uniaxial compression will be explained, which can well explain the two common types of failure in uniaxial compression. This work may enrich the basis research of rock mechanics.

2. Uniaxial Compression Mechanical Model of Cylindrical Rock Specimen

Figure 1 shows the uniaxial compression mechanical model of a typical cylindrical specimen, with the height$h$, the radius b, and the elastic modulus and Poisson's ratio E and μ, respectively. The rock mass deforms in both axial and radial directions when the uniformly distributed load σ_v is applied in the axial direction (since the volume force is much smaller than σ_v, the volume force is isotropic and not considered). Some researchers have found that the force exerted on the surface of the specimen by the testing machine is nonuniform. But in practice, if the specimen meets the requirements of flatness and straightness, the assumption of axial uniform pressure is approximately true. Furthermore, by applying lubricant on the contact surface, the friction effect

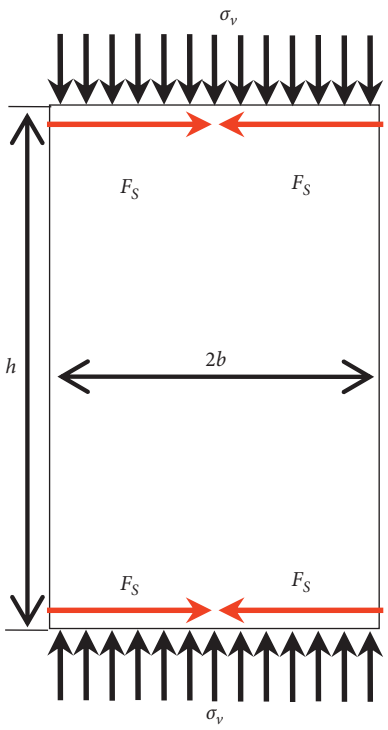

Figure 1: Uniaxial compression mechanics.

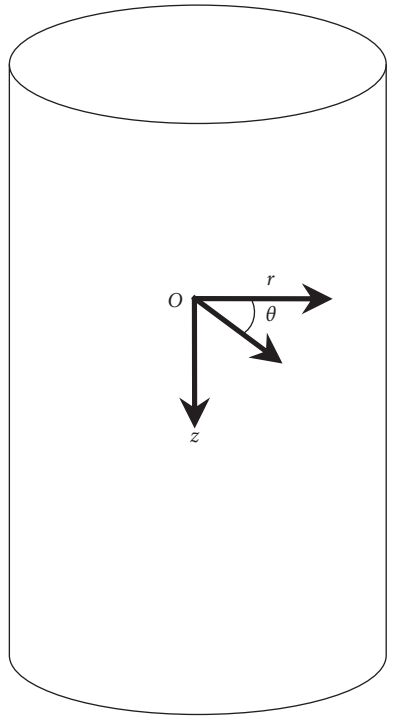

Figure 2: Cylindrical coordinate system model of rock specimen.

can be reduced and the uniformity of axial pressure can be further ensured. In the process of continuous deformation, the upper and lower surface of the rock specimen will produce friction binding force F_s, which is similar to the case in physics where the slider moves on a nonsmooth contact surface. In the limit case, when all the points at the same position on the two interfaces have relative motion, the value of F_s follows the friction law (take unit angle):

$$F_{s\max} = \frac{\sigma_v f b^2}{2}, \tag{1}$$

where $F_{s\max}$ is the maximum value of the derived friction binding force and 30° is the friction coefficient of the contact surface.

As shown in Figure 2, a space cylindrical coordinate system is established at the center of the specimen, with the z axis along the axial direction, the downward direction as the positive direction, and the r axis along the radial direction.

3. Stress Function

3.1. Stress Function Form Analysis. According to the basic theory of elastic mechanics, the stress function of space axisymmetric problem is a function that is only related to z and ρ, but unrelated to θ. Therefore, the stress function is expressed as $\phi_{(\rho,z)}$, and the terms can be expressed in the form of exponential function, logarithmic function, exponential function form, and so on. But according to the definition domain and its physical meaning, the exponential function with positive integer is selected as the term of the stress function. Suppose the stress function has the form as

$$\phi_{(\rho,z)} = \sum \rho^m z^n \, (m, n \in N). \tag{2}$$

The stress function $\phi_{(\rho,z)}$ must be a biharmonic function and satisfy the compatible equation $\nabla^4 \varphi = 0$. The term of the stress function is expressed as

$$F_{(\rho,z)} = \rho^m z^n \, (m, n \in N), \tag{3}$$

and

$$\begin{aligned}
\nabla^4 F_{(\rho,z)} &= m(m-1)(m-2)(m-3)\rho^{(m-4)} z^n + 2m(m-1)(m-2)\rho^{(m-4)} z^n \\
&\quad - m(m-1)\rho^{(m-4)} z^n + mr^{(m-4)} z^n + 2mn(m-1)(n-1)\rho^{(m-2)} z^{(n-2)} \\
&\quad + 2mn(n-1)\rho^{(m-2)} z^{(n-2)} + n(n-1)(n-2)(n-3)\rho^m z^{(n-4)} \\
&= m^2 (m-2)^2 \rho^{(m-4)} z^n + 2m^2 n(n-1)^2 \rho^{(m-2)} z^{(n-2)} \\
&\quad + n(n-1)(n-2)(n-3)\rho^m z^{(n-4)}.
\end{aligned} \tag{4}$$

Formula (4) shows that terms of the same degree can be substituted into the compatible equation to the same power, while terms of different degrees can be substituted into the compatible equation to different powers. Therefore, if the stress function ϕ satisfies the compatible equation, the combination of terms of the same degree must satisfy the compatible equation. When m (the exponent of ρ) is even and $F_{(\rho,z)}$ of the same power is substituted into the compatible equation, the results are linearly dependent. When the exponent m of ρ is odd and $F_{(\rho,z)}$ of the same power is substituted into the compatible equation, the results are linearly independent and the stress function cannot be constructed to satisfy the compatible equation. So, we know that the exponent of ρ has to be even.

From the terms of the stress function $F_{(\rho,z)}$, the terms of the stress component can be expressed as

$$\begin{aligned}
\sigma_{zF} &= \frac{\partial}{\partial z}\left[(2-\mu)\nabla^2 F_{(\rho,z)} - \frac{\partial^2 F_{(\rho,z)}}{\partial z^2}\right],\\
&= (2-\mu)\left[m^2 n\rho^{(m-2)}z^{(n-1)} + n(n-1)(n-2)\rho^m z^{(n-3)}\right] - n(n-1)(n-2)\rho^m z^{(n-3)},\\
&= (2-\mu)m^2 n\rho^{(m-2)}z^{(n-1)} + (1-\mu)n(n-1)(n-2)\rho^m z^{(n-3)},\\
\sigma_{\rho F} &= \frac{\partial}{\partial z}\left[\mu\nabla^2 F_{(\rho,z)} - \frac{\partial^2 F_{(\rho,z)}}{\partial \rho^2}\right],\\
&= \mu\left[m^2 n\rho^{(m-2)}z^{(n-1)} + n(n-1)(n-2)\rho^m z^{(n-3)}\right] - mn(n-1)\rho^{(m-2)}z^{(n-1)},\\
&= mn(\mu m - m + 1)\rho^{(m-2)}z^{(n-1)} + \mu n(n-1)(n-2)\rho^m z^{(n-3)},\\
\sigma_{\theta F} &= \frac{\partial}{\partial z}\left[\mu\nabla^2 F_{(\rho,z)} - \frac{1}{\rho}\frac{\partial F_{(\rho,z)}}{\partial r}\right],\\
&= \mu\left[m^2 n\rho^{(m-2)}z^{(n-1)} + n(n-1)(n-2)\rho^m z^{(-3)}\right] - mn\rho^{(m-2)}z^{(n-1)},\\
&= mn(\mu m - 1)\rho^{(m-2)}z^{(n-1)} + \mu n(n-1)(n-2)\rho^m z^{(n-3)},\\
\tau_{z\rho F} &= \tau_{\rho z F} = \frac{\partial}{\partial \rho}\left[(1-\mu)\nabla^2 F_{(\rho,z)} - \frac{\partial^2 F_{(\rho,z)}}{\partial z^2}\right],\\
&= (1-\mu)\left[m^2(m-2)\rho^{(m-3)}z^n + mn(n-1)\rho^{(m-1)}z^{(n-2)}\right] - mn(n-1)\rho^{(m-1)}z^{(n-2)},\\
&= (1-\mu)m^2(m-2)\rho^{(m-3)}z^n - \mu mn(n-1)(n-2)\rho^{(m-1)}z^{(n-2)}.
\end{aligned} \tag{5}$$

According to the z-axis symmetry of the specimen, it can be known that σ_z must be z-axis symmetric, that is, σ_z is an even function of z. n is odd by combining with formula (5). At this point, there is $F_{(\rho,z)} = \rho^m z^n (m, n \in N, m$ is even, and n is odd). Removing the independent stress term: z, which can be set

$$\begin{cases}
y_0 = A_0 z^3 + B_0 r^2 z,\\
y_1 = A_1 z^4 + B_1 r^2 z^2 + C_1 r^4\\
y_2 = A_2 z^5 + B_2 r^2 z^3 + C_2 r^4 z,\\
y_3 = A_3 z^6 + B_3 r^2 z^4 + C_3 r^4 z^2 + D_3 r^6,\\
y_4 = A_4 z^7 + B_4 r^2 z^5 + C_4 r^4 z^3 + D_4 r^6 z,\\
\vdots\\
y_k = A_k z^{2k+3} + B_k r^2 z^{2k+1} + C_k r^4 z^{2k-1} + \cdots, \quad (k \in N),
\end{cases} \tag{6}$$

there are

$$\phi_{(\rho,z)} = y_0 + y_2 + y_4 + y_6 + \cdots y_n \ (n \in N \text{ and } n \text{ is even}). \tag{7}$$

Substituting $y_0, y_2, y_4, \ldots, y_n$ into the compatible equation and combining formula (4), we have

$$\begin{cases}
\nabla^4 y_0 = 0,\\
\nabla^4 y_2 = (120A_2 + 48B_2 + 64C_2)z,\\
\nabla^4 y_4 = (840A_4 + 160B_4 + 64C_4)z^3\\
\quad +(120B_4 + 120C_4 + 480D_4)\rho^2 z,\\
\vdots\\
\nabla^4 y_n = \cdots.
\end{cases} \tag{8}$$

It can be known from the above that $y_0, y_2, y_4, \ldots, y_n$ is the biharmonic function. That is,

$$\begin{aligned} \nabla^4 y_0 &= 0, \\ \nabla^4 y_2 &= 0, \\ \nabla^4 y_4 &= 0, \\ \nabla^4 y_6 &= 0 \cdots \nabla^4 y_n = 0. \end{aligned} \tag{9}$$

Let

$$\begin{cases} \sigma_{z0} = \dfrac{\partial}{\partial z}\left[(2-\mu)\nabla^2 y_0 - \dfrac{\partial^2 y_0}{\partial z^2}\right], \\ \sigma_{z2} = \dfrac{\partial}{\partial z}\left[(2-\mu)\nabla^2 y_2 - \dfrac{\partial^2 y_2}{\partial z^2}\right], \\ \sigma_{z4} = \dfrac{\partial}{\partial z}\left[(2-\mu)\nabla^2 y_4 - \dfrac{\partial^2 y_4}{\partial z^2}\right], \\ \vdots \\ \sigma_{zn} = \dfrac{\partial}{\partial z}\left[(2-\mu)\nabla^2 y_n - \dfrac{\partial^2 y_n}{\partial z^2}\right]. \end{cases} \tag{10}$$

Substituting $y_0, y_2, y_4, \ldots, y_n$ into formula (10), we can get

$$\begin{cases} \sigma_{z0} = 6A_0(1-\mu) + 4B_0(2-\mu), \\ \sigma_{z2} = \left[60A_2(1-\mu) + 12B_2(2-\mu)\right]z^2 + \left[6B_2(1-\mu) + 16C_2(2-\mu)\right]\rho^2, \\ \sigma_{z4} = \left[210A_4(1-\mu) + 20B_4(2-\mu)\right]z^4 + \left[60B_4(1-\mu) + 48C_4(2-\mu)\right]\rho^2 z^2, \\ +\left[6C_4(1-\mu) + 36D_4(2-\mu)\right]\rho^4, \\ \vdots \\ \sigma_{zn} = \cdots. \end{cases} \tag{11}$$

In Figure 1, since F_S is the derived friction binding force, the direction is outward along the radius and the z direction of the sandwich contact surface is only subject to uniform distribution stress σ_v' actually, and the axial stress σ_z can be regarded as a function of z in the specimen, that is, σ_z is independent of ρ. According to formulae (8), (9), and (11), the conditions are right.

$$\text{When } k = 2, \begin{cases} 120A_2 + 48B_2 + 64C_2 = 0, \\ 6B_2(1-\mu) + 16C_2(2-\mu) = 0, \end{cases} \tag{12a}$$

$$\text{when } k = 4, \begin{cases} 840A_4 + 160B_4 + 64C = 0, \\ 120B_4 + 120C_4 + 480D_4 = 0, \\ 60B_4(1-\mu) + 48C_2(2-\mu) = 0, \\ 6C_4(1-\mu) + 36D_4(2-\mu) = 0, \end{cases} \tag{12b}$$

$$\vdots$$

$$\text{when } k = \cdots.$$

Solution to formula (12a) is obtained as follows:

$$A_2 = \frac{8(3-\mu)}{15(1-\mu)}C_2, \tag{13a}$$

$$B_2 = -\frac{8(2-\mu)}{3(1-\mu)}C_2. \tag{13b}$$

Solution to formula (12b) shows that the equation system can only be established if and only if all of A_4, B_4, C_4, and D_4 are equal to 0. It can be seen from the analysis that each increase of n by 2 will increase a coefficient in the function y_n, and two equations will be added to the corresponding equation system and generate excessive constraints in formulae (12a) and (12b). The equation system can only be established if and only if all the unknowns contained are 0, that is, when the conditions of $n > 2$cannot be satisfied. So, the stress function can be expressed as

$$\phi_{(\rho,z)} = y_0 + y_2 = A_0 z^3 + B_0 \rho^2 z + A_2 z^5 + B_2 \rho^2 z^3 + C_2 \rho^4 z. \tag{14}$$

The stress components can be expressed as

$$\sigma_z = 6A_0(1-\mu) + 4B_0(2-\mu) + \left[60A_2(1-\mu) + 12B_2(2-\mu)\right] z^2, \tag{15a}$$

$$\sigma_\rho = 6A_0\mu + 4B_0\mu - 2B_0 + \left[60A_2\mu + 6B_2(2\mu-1)\right] z^2 + \left[6B_2\mu + 4C_2(4\mu-3)\right]\rho^2, \tag{15b}$$

$$\sigma_\varphi = 6A_0\mu + 4B_0\mu - 2B_0 + \left[60A_2\mu + 6B_2(2\mu-1)\right] z^2 + \left[6B_2\mu + 4C_2(4\mu-1)\right]\rho^2, \tag{15c}$$

$$\sigma_z = 6A_0(1-\mu) + 4B_0(2-\mu) + \left[60A_2(1-\mu) + 12B_2(2-\mu)\right] z^2. \tag{15d}$$

3.2. Boundary Conditions. For the boundary conditions of rock mass specimens, the main boundary conditions should be exactly satisfied firstly, and the secondary boundary conditions should be satisfied as far as possible. The tension of normal stress is defined as "+," and the pressure is defined as "–" The sign for shear stress is defined as follows: when the specimen is clockwise rotation, the shear stress is defined as "+." For the counterclockwise rotation, the shear stress is defined as "–." Next, the boundary conditions are substituted into the parameters in formulae (14) and (15a)–(15d).

(1) The z-direction stress of the upper and lower end faces is $-\sigma_v'$:

$$\left((\sigma_z)_{z=-(h/2)} = -\sigma_v\right), \tag{16a}$$

$$(\sigma_z)_{z=(h/2)} = -\sigma_v. \tag{16b}$$

Formulae (16a) and (16b) can be obtained.

$$6A_0(1-\mu) + 4B_0(2-\mu) + \left[60A_2(1-\mu) + 12B_2(2-\mu)\right] \times \frac{h^2}{4} = -\sigma_v. \tag{17}$$

(2) Resultant force of shear stress is zero of lateral free surface (unit angle):
$\int_{-(h/2)}^{(h/2)} (\tau_{z\rho})_{\rho=b} \mathrm{d}z = 0$, natural meet.

(3) Resultant force of the shear stress of the upper and lower boundary, respectively, is F_S and $-F_S$ (taking unit angle).

Upper boundary:

$$\int_0^b \left(\tau_{\rho z}\right)_{z=-(h/2)} \rho \, \mathrm{d}\rho = F_S. \tag{18}$$

Reduction to draw:

$$\frac{2}{3}\left[3B_2\mu - 8C_2(1-\mu)\right] h b^3 = F_S. \tag{19}$$

Lower boundary:

$$\int_0^b \left(\tau_{\rho z}\right)_{z=(h/2)} \rho \, \mathrm{d}\rho = -F_S. \tag{20}$$

This simplifies to the same (3)–(17), (19), (21), and (23).

Formulae (3)–((15a)–(15d)) and formulae (3)–(17), (19), (21), and (23) can be calculated:

$$A_2 = -\frac{3-\mu}{10hb^3}F_S,$$

$$B_2 = \frac{2-\mu}{2hb^3}F_S, \tag{21}$$

$$C_2 = -\frac{3(1-\mu)}{16hb^3}F_S.$$

(4) The resultant of normal stress on the free side is zero:

$$\int_{-(\mathrm{h}/2)}^{(\mathrm{h}/2)} \left(\sigma_\rho\right)_{\rho=b} \mathrm{d}z = 0, \tag{22}$$

which reduces to

$$(6A_0\mu + 4B_0\mu - 2B_0)h + \left[5A_2\mu + B_2\left(\mu - \frac{1}{2}\right)\right] h^3 + \left[6B_2\mu + 4C_2(4\mu-3)\right] b^2 h = 0. \tag{23}$$

(5) The resultant moment of the free side is zero: $\int_{-(h/2)}^{(h/2)} (\sigma_\rho)_{\rho=b} z \mathrm{d}z = 0$, natural meet.

According to formulae (17) and (21), the following equation can be obtained:

$$6A_0(1-\mu) + 4B_0(2-\mu) + \frac{3h}{2b^3}F_S = -\sigma_v. \tag{24}$$

According to formulae (21) and (23), the following equation can be obtained:

$$6A_0\mu + 4B_0\mu - 2B_0 - \frac{(2+\mu)h}{4b^3}F_S + \frac{3(3+\mu)}{4hb}F_S = 0. \quad (25)$$

From formulae (24) and (25), we can get

$$\begin{aligned} A_0 &= \frac{(2-\mu)(2+\mu)h}{12b^3(\mu+1)}F_S - \frac{(3+\mu)(2-\mu)}{4hb(\mu+1)}F_S + \frac{(2\mu-1)h}{4b^3(\mu+1)}F_S + \frac{(2\mu-1)\sigma_v'}{6(\mu+1)}, \\ B_0 &= \frac{3(3+\mu)(1-\mu)}{8hb(\mu+1)}F_S - \frac{(2+\mu)(1-\mu)h}{8b^3(\mu+1)}F_S - \frac{3\mu h}{4b^3(\mu+1)}F_S - \frac{\mu\sigma_v'}{2(\mu+1)}. \end{aligned} \quad (26)$$

Thus, all undetermined coefficients are determined. The stress function and each stress component are determined accordingly, as shown in formulae (27) and (28), respectively.

$$\begin{aligned} \phi_{(z,\rho)} = &\left[\frac{(2-\mu)(2+\mu)h}{24b^3\mu}F_S - \frac{(3+\mu)(2-\mu)}{8hb\mu}F_S + \frac{h}{4b^3}F_S + \frac{\sigma_v'}{6} - \frac{1}{3} + \frac{2-\mu}{3\mu}\right]z^3 \\ &+ \left[\frac{3(3+\mu)(1-\mu)}{16hb\mu}F_S - \frac{(2+\mu)(1-\mu)h}{16b^3\mu}F_S - \frac{3h}{8b^3}F_S - \frac{\sigma_v'}{4} + \frac{1}{2} - \frac{1-\mu}{2\mu}\right]\rho^2 z \\ &- \frac{(3-\mu)F_S}{10hb^3}z^5 + \frac{(2-\mu)F_S}{2hb^3}\rho^2 z^3 - \frac{3(1-\mu)F_S}{16hb^3}\rho^4 z. \end{aligned} \quad (27)$$

$$\begin{aligned} \sigma_z &= \frac{6F_S}{hb^3}z^2 - \frac{3F_S h}{2b^3} - \sigma_v', \\ \sigma_\rho &= \frac{3(\mu+3)F_S}{4hb^3}\rho^2 - \frac{3(\mu+2)F_S}{hb^3}z^2 + \frac{(2+\mu)F_S h}{4b^3} - \frac{3(3+\mu)F_S}{4hb}, \\ \sigma_\theta &= \frac{3(3\mu+1)F_S}{4hb^3}\rho^2 - \frac{3(\mu+2)F_S}{hb^3}z^2 + \frac{(2+\mu)F_S h}{4b^3} - \frac{3(3+\mu)F_S}{4hb}, \\ \tau_{z\rho} &= \tau_{\rho z} = -\frac{6F_S}{hb^3}\rho z. \end{aligned} \quad (28)$$

4. Uniaxial Compression Stress Distribution of Cylindrical Rock Specimens

In order to directly reflect the results, the assignment calculation is adopted based on experience and standard. If the standard cylinder specimen is taken and the height-diameter ratio is equal to2: 1, then H = 4b, that is, the full height of the specimen H = 100 mm, the radius b = 25 mm, the modulus of elasticity E = 800 MPa, uniformly distributed axial load σ_v = 2 MPa, Poisson's ratioμ = 0.28, friction coefficient between specimen and end face f = 0.21, and maximum frictional force $F_f = (\sigma_v f b^2/2)$. All these can be substituted into the stress component expression (28), which can be further simplified to

$$\begin{aligned} \sigma_z &= 0.000504z^2 - 3.26, \\ \sigma_\rho &= 0.00020664\rho^2 - 0.00057456z^2 + 0.34965, \\ \sigma_\varphi &= 0.00011592\rho^2 - 0.00057456z^2 + 0.34965, \\ \tau_{z\rho} &= -0.000504\rho z. \end{aligned} \quad (29)$$

Because $\tau_{\rho\varphi} = \tau_{\varphi\rho} = \tau_{z\varphi} = \tau_{\varphi z} = 0$, σ_φ can be thought of as a principal stress, and the stresses on the cross sections orthogonal to the principal plane are independent of the principal stress σ_φ. Therefore, the three-dimensional problem can be transformed into a plane problem, combined with the calculation formula of plane principal stress:

$$\begin{matrix}\sigma_1 \\ \sigma_3\end{matrix} = \frac{\sigma_z + \sigma_\rho}{2} \pm \sqrt{\left(\frac{\sigma_z - \sigma_\rho}{2}\right)^2 + \tau_{z\rho}^2}, \quad (30)$$

and if specific values are substituted, Table 1 can be obtained.

The following conclusions can be drawn from the analysis of formulae (28) and (29):

(1) The stress component at different positions of rock specimen is related to the uniform load applied, the friction coefficient between the specimen and the applied force, and the height-diameter ratio of the specimen. Among them, $\sigma_\rho$and $\sigma_\varphi$are also related to Poisson's ratio of the specimen. The greater the applied load, the greater the stress component.

(2) The normal stress of rock specimen has a quadratic function relation with the height and diameter of the specimen, and the shear stress has a linear function

Table 1: Stress distribution details of sample internal key points (unit of stress: MPa).

z	$f = 0.21, \mu = 0.28, \sigma_v' = 2$ Mpa	ρ 0	$(b/2)$	b
$-(h/2)$	σ_z	−2	−2	−2
	σ_ρ	1.0868	−1.0545	0.9576
	σ_φ/σ_2	−1.0868	−1.0686	1.0143
	$\tau_{z\rho}$	0	0.315	0.63
	σ_1	−1.0868	−0.9592	−0.5284
	σ_3	−2	−2.0953	−2.4276
$-(h/4)$	σ_z	−2.945	−2.945	−2.945
	σ_ρ	−0.0095	0.0228	0.1197
	σ_φ/σ_2	−0.0095	0.00866	0.063
	$\tau_{z\rho}$	0	0.1575	0.315
	σ_1	−0.0095	0.0311	0.1517
	σ_3	−2.945	−2.9533	−2.977
0	σ_z	−3.26	−3.26	−3.26
	σ_ρ	0.3497	0.3819	0.4788
	σ_φ/σ_2	0.3497	0.3678	0.4221
	$\tau_{z\rho}$	0	0	0
	σ_1	0.3497	0.3819	0.4788
	σ_3	−3.26	−3.26	−3.26
$(h/4)$	σ_z	−2.945	−2.945	−2.945
	σ_ρ	−0.0095	0.0228	0.1197
	σ_φ/σ_2	−0.0095	0.00866	0.063
	$\tau_{z\rho}$	0	−0.1575	−0.315
	σ_1	−0.0095	0.0311	0.1517
	σ_3	−2.945	−2.9533	−2.977
$(h/2)$	σ_z	−2	−2	−2
	σ_ρ	−1.0868	−1.0545	−0.9576
	σ_φ/σ_2	−1.0868	−1.0686	−1.0143
	$\tau_{z\rho}$	0	−0.315	−0.63
	σ_1	−1.0868	−0.9592	−0.5284
	σ_3	−2	−2.0953	−2.4276

distribution with the height and diameter of the specimen.

By comparing Table 1 and above, more accurate conclusions can be drawn:

(1) All normal stress components and principal stress are distributed symmetrically around the surface $\rho o\varphi$.

(2) Normal stress σ_z is compression stress, which is the smallest at both ends of the specimen and the largest in the middle of the specimen, whose value is not related to ρ.

(3) The existence of friction force is like a hoop applied to the specimen. The normal stress presents a compression distribution at both ends from $(h/4)$ to $(h/2)$ of the specimen. The closer the same height is to the center, the greater the absolute value of the stress will be. Just as stress accumulates from all sides towards the center, stress is in the tensile state from the middle of $(h/4)$ to $(h/4)$, and the outward tensile stress at the same height increases.

(4) The absolute value of normal stress is relatively large from $(h/2)$ to $\pm(h/4)$ at both ends of the specimen, while the stress at $\pm(h/4)$ is small and almost negligible. But it gets bigger in the opposite direction at $h = 0$.

(5) The tangential stress is distributed in mirror image on $\rho o\varphi$ plane, whose absolute value increases with the increase of the absolute value of h andρ. It indicates that the closer the specimen is to the surface, the greater the shear stress will be. The shear stress is zero at $z = 0$ or $\rho = 0$. In summary, due to the existence of friction force, the stress value of the specimen is distributed centrally at both ends, which leads to complicated stress situation at both ends. The direction of stress will also change along the direction of height and radial direction.

(6) By analyzing the maximum principal stress, it can be found that the absolute value of maximum principal stress increases from both ends of the rock mass to the middle, which reaches the maximum value at the middle height of the rock mass, and is equal to σ_z in value.

(7) The distribution of minimum principal stress $\sigma_\varphi$is similar to the above. It indicates that the direction of principal stress of rock mass is consistent with the direction of coordinate axes at $h = 0$. The place of

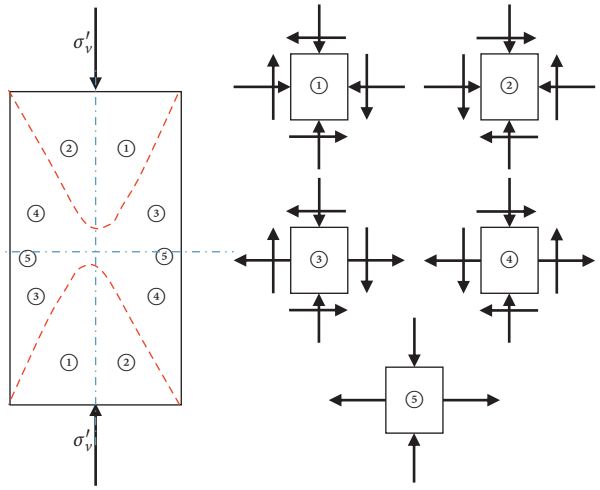

Figure 3: Stress distribution of uniaxial compression specimen considering friction.

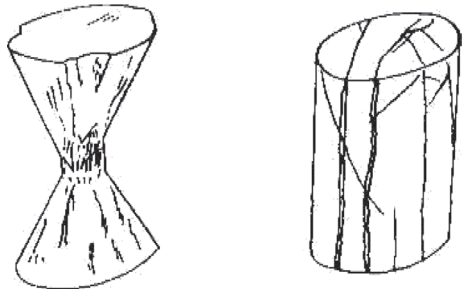

Figure 4: Two common failure modes of rock under uniaxial compression.

$h = 0$ and $\rho = b$ is the place where rock mass is most prone to failure.

According to Mohr criterion, bidirectional compressive strength > unidirectional compressive strength > bidirectional tensile strength. Therefore, considering the friction, the specimen in the zones of ① and ② forms a tight hoop effect, not easy to damage, while the specimen in the ⑤ zone damages first (the radius of the stress circle is the maximum, bidirectional tensile), and the damage extends to the zones of ③ and ④ and forms the conical failure pattern (namely, the conjugate shear failure surface under Mohr–Coulomb criterion), as shown in Figure 3. This is consistent with the common failure patterns of uniaxial compression specimens.

$F_S = 0$ when the friction effect at the end is not considered. Formula (28) can be further reduced to

$$\begin{aligned} \sigma_Z &= -\sigma_v', \\ \sigma_\rho = \sigma_\theta &= \tau_{z\rho} = \tau_{\rho z} = 0. \end{aligned} \tag{31}$$

Obviously, each point is a unidirectional stress state, and σ_z is the main stress. In the transverse direction, due to the Poisson effect, the lateral strain is generated. The strain is the same at the same ρ position. When the strain reaches the maximum of elongation line strain, it will crack along the parallel direction of the main stress. Considering the inevitable nonuniformity of the material, the cracks may be multiple and finally present the splitting failure pattern. In this way, logical and reasonable explanations are given for the causes of the two kinds of failure modes commonly seen in uniaxial compression experiments of rock specimens (see Figure 4).

The compressive strength is always obtained by $\sigma_c = (F/A)$ in standard rock compression experiments, provided that each point inside the specimen is in a unidirectional stress state. In fact, the points in the specimen are not in a unidirectional stress state when the friction effect of the end is considered. Obviously, the unidirectional stress state can only be approximately considered when the specimen is prepared in full compliance with national standards and the end face is treated with special lubrication during loading.

Data Availability

The data used to support the findings of this study are available from the corresponding author upon request.

Conflicts of Interest

The authors declare that they have no conflicts of interest.

Acknowledgments

The authors gratefully acknowledge the financial support from the Natural Science Foundation of Shandong Province (ZR2019MEE082).

References

[1] H. Yin and M. Wang, "Stress functions in two-dimensional, three-dimensional and *n*-dimensional elasticity," *Acta Scientiarum Naturalium Universitatis Pekinensis*, vol. 1, pp. 23–28, 1998.

[2] L. Chen, "The three dimension stress function," *Journal of Taiyuan University of Technology*, vol. 4, pp. 436–440, 2001.

[3] S. P. Timoshenko and J. N. Goodier, *Theory of Elasticity*, Higher Education Press, Beijing, China, 3rd edition, 2013.

[4] Z. Xu, *Elasticity*, Higher Education Press, Beijing, China, 3rd edition, 1990.

[5] J. Liu and Y. Zeng, "Numerical simulation of the end frictional effect of rock specimens," *Journal of Engineering Geology*, vol. 02, pp. 247–251, 2005.

[6] J. Li, *Study on Strength and Creep Characteristics of Composite Rock Mass with Inclined Soft-Weak Interlayer*, Qingdao University of Science and Technology, Qingdao, China, 2015.

[7] Y. Fang, Y. Liu, Q. Miao et al., "Analysis of gravity retaining wall based on semi-inver- se solution," *Low Temperature Architecture Technology*, vol. 38, no. 7, pp. 135–137, 2016.

[8] Y. Lao, "A direct method for finding the stress function," *Public Communication of Science & Technology*, vol. 8, no. 10, pp. 125-126, 2016.

[9] C. Zhang, J. Zhang, M. Ke et al., "Analysis of composite material thick walled tubes subjected to pure bending loading using two stress functions independent to each other," *Journal of Xiamen University (Natural Science)*, vol. 56, no. 6, pp. 900–906, 2017.

[10] J. Wu, S. Chen, and J. He, "Stress function analytic method for initial stress fields of rock masses with strata interfaces," *Journal of Central South University(Science and Technology)*, vol. 45, no. 11, pp. 3922–3929, 2014.

[11] Y. Hou, S. Duan, and R. An, "A semi-analytical method for stress functions meeting crack opening displacements in fracture process zones," *Applied Mathematics and Mechanics*, vol. 39, no. 8, pp. 979–988, 2018.

[12] B. Gai, "On axial-symmetrical space problems in elasticity and the general solution for *n*-fold quasi-harmonic equation," *Journal of Harbin Institute of Technology*, vol. 2, pp. 95–101, 1993.